Received July 8, 2019, accepted July 22, 2019, date of publication August 1, 2019, date of current version August 30, 2019.

Digital Object Identifier 10.1109/ACCESS.2019.2932507

An Improved SOC Estimator Using Time-Varying Discrete Sliding Mode Observer

KANGWEI DAI, JU WANG, AND HONGWEN HE, (Senior Member, IEEE)

National Engineering Laboratory for Electric Vehicles, School of Mechanical Engineering, Beijing Institute of Technology, Beijing 100081, China

Corresponding author: Ju Wang (wang_ju@bit.edu.cn)

This work was supported in part by the National Key Research and Development Program of China under Grant 2017YFB0103802, and in part by the Graduate Technological Innovation Project Beijing Institute of Technology under Grant 2018CX10003.

ABSTRACT Accurate estimations of battery state of charge (SOC) are great of significance for achieving stable and safe operation of electric vehicles. To meet the requirement of high robustness and real-time, the sliding mode observer with linear time-invariant battery model is usually used to estimate SOC of batteries. However, the observer for state estimation based on the time-varying model is rarely. In addition, there is a lack of stability proof for observers with time-varying systems. The applicability of the observer in different types of batteries is yet to be discussed. The application accuracy of the observer in the battery management system (BMS) needs to be further verified. To solve these issues, an improved observer-based estimation algorithm has been proposed. In this paper, a recursive fitting technology is used to automatically update the variable parameters of the battery, then the time-varying-model-based discrete sliding mode observer (TVDSMO) is proposed to build a SOC estimator. The stability condition is proposed to online evaluate the presented observer. The presented estimator has been verified by LiFePO4 (LFP) and Ni-Mn-Co (NMC) lithium-ion cells under different operating temperatures and working conditions. Finally, a platform based hardware-in-loop is built to verify the proposed method. The result manifests that the maximum estimation errors of SOC are both within 4% for NMC and LFP cells when the erroneous initial value of SOC and capacity are both considered. Additionally, the results from the platform show that the SOC estimation error is less 4.6% which fully meets the application of BMS.

INDEX TERMS Lithium-ion battery, state of charge, discrete stability condition, time-varying-model-based discrete sliding mode observer, BMS.

I. INTRODUCTION

As the developing tendency of global energy energy turning to new energy, lithium-ion batteries (LIB) are widely used in the field of transportations and stored energy due to the advantages of high energy density, high power density and low cost [1], [2]. An accurate SOC is an essential indicator for LIB safety and durability management in electric vehicles. However, because of the uncertain noises and nonlinear behaviors affected by internal aging and external conditions, a precise and reliable SOC estimation still remains big challenges for BMS [3]. Therefore, it is practical and of positive significance for the persistent improvement of SOC accuracy.

The associate editor coordinating the review of this manuscript and approving it for publication was Gaetano Zizzo.

A. STATE OF THE ART OF ESTIMATION APPROACHES

The existing methods for SOC estimation can be grouped into four categories in view of calculation theories, namely, ampere-hour integration, look-up table based methods, modern control theory based estimation and data-driven approaches [3], [4]. The most traditional method to estimate SOC is the ampere-hour integration (AHI) with the least computational complexity, whose evaluated error is more than 20% due to the uncertain initial value, inaccurate maximum available capacity, and the noises of current sensors [5]. The open circuit voltage (OCV) is usually used to modified SOC because of the monotonous mapping relationship existing between them. Whereas, the calculation error of this methods is greater than 5%, comprehensively affected by the aging, surrounding temperature, hysteresis behaviors and measuring errors [6]. Currently, the impacts of temperature and aging on the OCV-SOC curve are studied by some

researchers [7], [8]. This method has two main disadvantages: the long resting time and the high-accuracy measurement of voltage [9], [10]. The data-driven methods are intelligent methods by using the black-box model to accurately fit the strong time-variable relationship between the states and input variables [11]. The accuracy of these methods depends on the completeness of training data. However, as the uncertainty of application condition exists, these methods may be unfit for real-time controllers in vehicles right now.

The modern control theory based methods for SOC estimation are hot topics. The main core processes are feedback and modification. These methods can be divided into Kalman Filters (KF) based family and state observers based family in view of the feedback gain [8], [12]. The KF family for SOC estimation includes extended Kalman Filter (EKF) [13], adaptive EKF [14], unscented Kalman filter [15], and H infinity filter (HIF) [16]. After knowing the information of models and measurement noises, the SOC error can be within 3% with unknown true state value [13]. But the calculation time of the KF algorithm is three times than the observer-based methods. It will increase the cost of the BMS due to the high-speed microcontroller used in circuit design. Consequently, the observer-based methods are more suitable for low-cost BMS.

B. LITERATURE REVIEW

Compared to the KF, the state observers not only have the less computation, but can achieve the exact SOC estimation considering the uncertain initial errors, measurement errors and model errors. These approaches are able to be split into three categories, in the case of observer structure, namely, proportional-integral observer (PIO) [12], Luenberger observer (LO) [16], sliding-mode observer (SMO) [17]–[19]. The PIO and LO are both used to estimate accurate SOC within 4% by using linear time-invariant battery models with the true capacity, which hardly meets the actual condition of aging and variant temperatures in the EVs. Because of the strong ability to suppress noise disturbance, the SMO is especially suitable for battery SOC estimation with nonlinear parameters [20]. Although the equivalent circuit model has been studied for more than 15 years, it still has the research value due to its strong real-time performance, great application potential and high fitting accuracy in common SOC range. At present the research based on equivalent circuit model and observer mainly focuses on the improvement of observer structure and mode. W. Li *et al.* proposed the discrete-time nonlinear observer to achieve SOC estimation, however the model parameters are determined by offline data [21]. J. Du *et al.* presented a sliding mode observer with adaptive gain, the second order RC model without updating parameters is used. The error of estimated SOC is within 5% [22]. To improve the accuracy of SOC, Q. Zhong *et al.* adopted the fractional order model. The high precision estimation of SOC is realized by combining sliding mode observation [23]. However, due to the nonlinear characteristics of the fractional order, the off-line data can only be used to build this model. Therefore, the application in engineering is obviously restricted. B. Ning *et al.* adopted a moving average filter to enforce the parameter identification for the Thevenin model [24]. Compared with the recursive least squares (RLS), this identification method has the characteristics of big storage and high calculated amount, so it does not improve the real-time performance of the algorithm. Z. Wei *et al.* proposed the bias compensating recursive least squares to achieve online parameter identification. The SOC is further estimated in real time by the Luenberger observer [25]. However, there are few researches on discrete SMO based on the strong real-time update of model parameters.

C. MOTIVATION AND INNOVATION

Since the parameters of battery will change at different temperatures and capacity degradation, it's very necessary to design an improved SMO with time-varying model to increase the accuracy of SOC estimation. At the same time, the application of proposed methods need be clearly illuminated in the estimation accuracy of different battery material systems. The proof of the stability of the time-varying system should be done. In addition, the application accuracy of this method in the real-time controller is also blurry.

To resolve the issues and validate the stability and performance of engineering application. We have made the following efforts: (1) An improved time-varying-model-based discrete sliding mode observer is proposed to build SOC estimator. The details of the algorithm running process are demonstrated. (2) we propose the sliding stability condition of the discrete system to validate the stability of the TVDSMO and the online operation stability is firstly calculated according to the working conditions. (3) In order to validate the accuracy of this method, we compare it with DSMO after considering the erroneous initial SOC, incorrect capacity and cell types. To verify the engineering applicability of the algorithm, we build a test bench based on the real BMS.

D. ORGANIZATION OF THE PAPER

The organization of this paper is as follows. Section 2 illustrates the model of battery and the parameter online identification method. Section 3 describes the design processor of TVDSMO. We also introduce more details about how to use it in the BMS. Then, experiments of battery and validations of presented approach are demonstrated in Section 4. Finally, Section 5 demonstrate the main conclusions.

II. BATTERY MODELLING

A. LUMPED PARAMETERS BATTERY MODEL

The LiB has a very complex electrochemical behavior with electro-thermal coupling processes and some nonlinear characteristics. Its external characteristic behavior is described by the following equations:

$$U_t = U_{oc} - U_D - I_L R_o \tag{1}$$

$$\dot{U}_D = -\frac{1}{\tau_D}U_D + \frac{1}{C_D}I_L \tag{2}$$

where U_t is the terminal voltage. U_{oc} denotes the OCV. U_D is the polarization voltage. R_o is the ohmic resistance. I_L is the load current (assumed positive for discharge, negative for charge). The RC network including polarization resistance (R_D) and polarization capacitance (C_D), is used to describe electron diffusion and migration. τ_D is the diffusion constant, $\tau_D = R_D C_D$. The dynamic voltage is demonstrated by the following equation.

$$U_D = Ce^{-\int \frac{1}{\tau}dt} + e^{-\int \frac{1}{\tau}dt}\int \frac{I_L}{C_D}e^{-\int \frac{1}{\tau}dt}dt \tag{3}$$

where C is a constant value determined by the initial state. Assuming $U_{D,k+1}|_{\Delta t=0} = U_{D,k}$ as its initial value, Eq.(3) can be deduced by the following equation.

$$U_{D,k+1} = U_{D,k}\exp\left(-\Delta t/\tau_D\right) + \left[1-\exp\left(-\Delta t/\tau_D\right)\right]R_D I_{L,k} \tag{4}$$

where Δt denotes the sampling interval determined by the BMS. $U_{D,k+1}$ and $U_{D,k}$ denote the polarization voltage at time t_{k+1} and t_k, respectively. We define $E_t = U_t - U_{oc}$. U_{oc} can be calibrated by the SOC estimation algorithm. Consequently, Eq.(2) can be reconstructed by the following equation.

$$E_{t,k} = -U_{D,k} - I_{L,k}R_o \tag{5}$$

Combining with Eq.(4), the Eq.(5) can be deduced as Eq.(6).

$$E_{t,k+1} = -U_{D,k}\exp\left(-\Delta t/\tau_D\right) - \left[1-\exp\left(-\Delta t/\tau_D\right)\right]R_D I_{L,k} - I_{L,k+1}R_o \tag{6}$$

With further derivation:

$$E_{t,k+1} = \exp\left(-\frac{\Delta t}{\tau_D}\right)E_{t,k} - R_o I_{L,k+1} + (\exp(-\Delta t/\tau_D)R_o - (1-\exp\left(-\Delta t/\tau_D\right))R_D)I_{L,k} \tag{7}$$

Then the following equation is derived :

$$E_{t,k+1} = a_1 E_{t,k} + a_2 I_{L,k+1} + a_3 I_{L,k} \tag{8}$$

where a_1, a_2, a_3 are shown as follows:

$$a_1 = \exp\left(-\Delta t/\tau_D\right) \tag{9}$$

$$a_2 = -R_o \tag{10}$$

$$a_3 = \exp\left(-\Delta t/\tau_D\right)R_o - \left(1-\exp\left(-\Delta t/\tau_D\right)\right)R_D \tag{11}$$

Then the parameters of the battery model can be solved by the following equations:

$$R_D = \frac{a_1 a_2 + a_3}{a_1 - 1} \tag{12}$$

$$C_D = \frac{(1-a_1)\Delta t}{(a_1 a_2 + a_3)\log(a_1)} \tag{13}$$

Based on the format of the auto regressive exogenous algorithm, the electrical equation of the battery model can be reconstructed as follows:

$$y_k = \phi_k \theta_k + \sigma \tag{14}$$

where ϕ_k and θ_k denote data matrix and the parameter vector respectively. σ is the model error determined by the measurement noise. And the two vectors are shown by the following equations:

$$\phi_k = [\,E_{t,k-1} \quad I_{L,k} \quad I_{L,k-1}\,] \tag{15}$$

$$\theta_k = \left[\,a_1 \quad a_2 \quad a_3\,\right]^T \tag{16}$$

The state-space expression of the model can be described as:

$$U_{D,k+1} = \exp\left(-\Delta t/\tau_D\right)U_{D,k} + \left(1-\exp\left(-\Delta t/\tau_D\right)\right)R_D I_{L,k} \tag{17}$$

$$U_{t,k+1} = U_{oc,k+1} - U_{D,k+1} - R_o I_{L,k+1} \tag{18}$$

B. IDENTIFICATION METHOD

The recursive least squares algorithm has been adopted to execute the adaptive parameter identification for the model. The detailed computational processes of the model parameters are demonstrated in Table 1.

TABLE 1. The iteration procedure of recursive least squares algorithm [8].

(1) Initialization for the RLS parameters $\hat{\theta}_0, P_0, \lambda$
(2) Battery data measurement
Calculating ϕ_k the by Eq.(15) for next step
(3) Calculating the error covariance matrix P_k and gain matrix K_k.

$$P_k = \frac{P_{k-1} - K_k\phi_k^T P_{k-1}}{\lambda} \tag{19}$$

$$K_k = \frac{P_{k-1}\phi_k^T}{\lambda + \phi_k^T P_{k-1}\phi_k} \tag{20}$$

(4) Calculating model prediction error and update the parameters of model.

$$\varepsilon_k = y_k - \phi_k\hat{\theta}_k \tag{21}$$

$$\hat{\theta}_k = \hat{\theta}_{k-1} + K_k\varepsilon_k \tag{22}$$

(5) Computation the predicted terminal voltage and model parameters

$$U_{t,k} = U_{oc,k} + E_{t,k} \tag{23}$$

where λ is the forgetting factor for alleviating the influence from the previous measured data gradually.

III. BATTERY SOC ESTIMATOR

A. THE DESIGNING PROCESS FOR THE OBSERVER

The section introduces the necessary theory for the method proposed in this paper. Consider the following discrete system:

$$x_{k+1} = A_k x_k + B_k u_k + \omega_k \tag{24}$$

$$y_k = C_k x_k + D_k u_k + \nu_k \tag{25}$$

where x_k is the state vector, A_k is the system matrix, B_k denotes the input matrix, C_k denotes the observer matrix and D_k denotes the feedforward matrix. ω_k denotes the system noise, ν_k is the noise of measurement and disturbance. Assume the discrete system is observable in this paper. The traditional SMO has a dominant chattering, when reaching the sliding boundary [26]. We use the Walcott-Zak form

to abate the disadvantage. Its standard form is shown as following:

$$\hat{x}_{k+1} = A_k\hat{x}_k + B_k u_k + L\tilde{e}_{y,k} + Msat(\tilde{e}_{y,k}/\varphi) \quad (26)$$
$$\hat{y}_k = C_k\hat{x}_k + D_k u_k \quad (27)$$
$$\tilde{e}_{y,k} = y_k - \hat{y}_k \quad (28)$$

where $\hat{x}_k$ denotes the estimated value of state vector. $\hat{y}_k$ denotes predicted value of measurement. $\tilde{e}_{y,k}$ is the error of output. L and M are feedback gain and saturation gain, respectively. φ the means the sliding boundary. The $sat()$ is the saturation function.

$$sat(\varepsilon) = \begin{cases} \varepsilon, & -1 < \varepsilon < 1 \\ sgn(\varepsilon), & \varepsilon < -1,\ \varepsilon > 1 \end{cases}$$

where $sgn()$ is the sign function.The error of estimated state is defined by the following equations.

$$\tilde{x}_{k+1} = [A - LC]\tilde{x}_k + \Delta_k - Msat(C\tilde{x}_k/\varphi) \quad (29)$$
$$\tilde{x}_k = \hat{x}_k - x_k \quad (30)$$
$$\Delta_k = \omega_k + L\nu_k \quad (31)$$

For the DSMO shown by the equations above, the following condition must be satisfied [27]:

(1) The Δ_k and ν_k must be bounded by a known quantity Δ_λ and ν_λ, respectively.
(2) The saturation gain M must satisfy this condition: $M_i \geq \Delta_{\lambda,i}, i = 1 \ldots n$.
(3) The sliding boundary φ must satisfy this condition: $\varphi \geq \nu_\lambda$

According the stability condition for discrete sliding mode system presented by Sarpturk *et al.* [28], the system must satisfy the following condition:

$$[\tilde{x}_{k+1,i} + \tilde{x}_{k,i}]sgn(\tilde{x}_{k,i}) \geq 0, \quad i = 1 \ldots n \quad (32)$$

B. TIME-VARYING-MODEL-BASED SOC ESTIMATOR WITH DSMO

The standard form of the model is chosen to describe the dynamic character for LIBs. According to the Eq.(4) and the discrete SOC definition, the state equations is demonstrated as following:

$$x_{k+1} = A_k x_k + B_k I_{L,k} + \omega_k \quad (33)$$
$$U_{t,k} = C_k x_k + D_k + \nu_k \quad (34)$$

where $x_k = [U_{D,k} SOC_k]^T$, $A_k = \begin{bmatrix} e^{-\frac{\Delta t}{\tau_{Dk}}} & 0 \\ 0 & 1 \end{bmatrix}$, $B_k = [(1 - e^{-\frac{\Delta t}{\tau_{D,k}}})R_{D,k} \quad -\frac{\eta_{i,k}\Delta t}{C_a}]^T$, $D_k = U_{ocv,k} - R_{o,k}I_{L,k}$ $C_k = \begin{bmatrix} -1 & \frac{\partial U_{ocv,k}}{\partial z} | z = z_k \end{bmatrix}$. As the coulombic efficiency is up to 99.9% [29], the $\eta_{i,k}$ is set to 1 in this paper. The capacity of battery C_a is not the rated capacity in this paper, because it will change as the aging, surrounding temperature, loading conditions. Consequently, C_a is a dynamic value. Additionally, we sometimes use z to denote SOC for conciseness.

According to the form of DSMO designed in the last subsection, the TVDSMO-based SOC estimator is established.

$$\hat{x}_{k+1} = A_k\hat{x}_k + B_k I_k + L\tilde{e}_{y,k} + Msat(\tilde{e}_{y,k}/\varphi) \quad (35)$$
$$\hat{U}_{t,k} = C_k\hat{x}_k + \hat{U}_{ocv,k} - R_{o,k}I_{L,k} \quad (36)$$
$$\tilde{e}_{y,k} = U_{t,k} - \hat{U}_{t,k} \quad (37)$$

To ensure the robustness, the designed observer must satisfy the condition of stability. We take an example for analyzing stability in term of SOC, one of the states in this model. According to the stability condition for discrete system, the battery SOC estimator must meet it to ensure the stability during the algorithm operating.

$$z_{k+1} = z_k - \frac{\Delta t I_{L,k}\eta_{i,k}}{C_{a,k}} \quad (38)$$
$$\widehat{z}_{k+1} = \widehat{z}_k - \frac{\Delta t I_{L,k}\eta_{i,k}}{C_{a,k}} + L_1\tilde{e}_{y,k} + M_1 sat(\frac{\tilde{e}_{y,k}}{\varphi}) \quad (39)$$
$$\tilde{e}_{s,k} = \widehat{z}_k - z_k \quad (40)$$
$$[S(k+1) + S(k)]\, sgn\,[S(k)] = [2\tilde{e}_{s,k} + L_1\tilde{e}_{y,k} + M_1 sat(\frac{\tilde{e}_{y,k}}{\varphi})]sgn[\tilde{e}_{s,k}] \quad (41)$$

The L_1 and M_1 must always meet the following conditions: (1) If the $\tilde{e}_{s,k} > 0$, the $2\tilde{e}_{s,k} + L_1\tilde{e}_{y,k} + M_1 sat(\frac{\tilde{e}_{y,k}}{\varphi}) > 0$. (2) If the $\tilde{e}_{s,k} < 0$, the $2\tilde{e}_{s,k} + L_1\tilde{e}_{y,k} + M_1 sat(\frac{\tilde{e}_{y,k}}{\varphi}) < 0$.

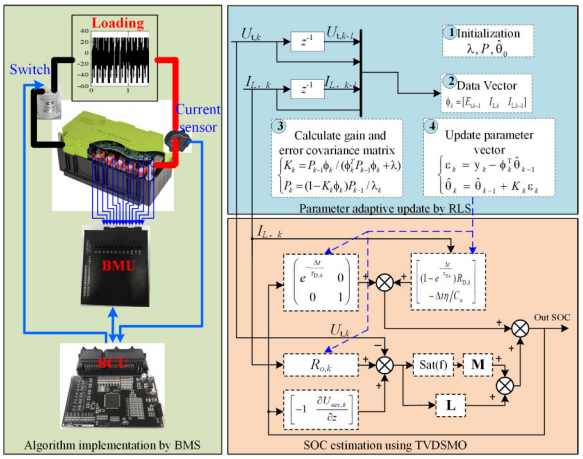

FIGURE 1. The implementation procedure of this joint framework.

C. MODEL-BASED ADAPTIVE PARAMETER AND SOC JOINT ESTIMATOR

When the presented algorithm used in the real-time controller, two essential steps must be paid attention, as shown in Fig.1. Step 1 is to determine what the structure is in the hardware system. Assuming that the typical BMS includes two controller units, battery monitor unit (BMU) and battery control unit (BCU). The BMU is responsible for information measurements such as voltages and temperatures of cells. Usually, battery packs are equipped with many BMUs for

information monitoring. The SOC estimation algorithm and other management strategies run in the BCU [30].

Normally, the BCU has an excellent processor, used to execute algorithms and control strategies. The implementation of SOC algorithm exists two processes in BCU. Firstly, the battery information is measured via BMU according to a certain sampling frequency, such as 10Hz. Then the BMU transmits these data to the bus of the controller area network (CAN) according to a standard of communication protocol, such as ISO11898 and ISO11519-2. Then, the BCU periodically accepts the CAN message including cell voltage and temperature. It reads the current from busbar of battery pack. Then the SOC algorithm in a timer process is implemented in the light of a certain period such as 0.1s or 1s.

Step 2 is to implement the presented method to estimate SOC. Firstly, the parameters adopted in this algorithm need to be initialized. The $\hat{\theta}_0$ equals to $[0, 0, 0]$. The covariance matrix P_0 is set to a diagonal matrix, whose diagonal values are the same, set to 10^6. The forgettable factor of the RLS is set to 0.985. The feedback gain and saturation gain are optimized by the genetic algorithm, which simultaneously meets the stability condition. The sliding boundary φ is determined by the measurement error. It is set to 0.005 in this paper. Secondly, the iteration of RLS is executed. The voltage and current are collected to construct the data vector. Then the gain and covariance matrix are calculated. Finally, the parameter vector is updated. The iteration of TVDSMO is carried out according to Eq.(38)-(40).

IV. VERIFICATION AND DISCUSSION

This section mainly verifies the proposed approach. To acquire the battery date, we need to build a platform for experiment.

A. EXPERIMENT

The battery testing bench consists of four parts: (1) Arbin BT2000: it is employed to stimulate battery via using the designed the loading profiles and collect the real-time data. (2) Environmental test chamber: it is used to simulate operation temperature of the battery. (3) Battery: LiFePO4 lithium-ion battery and Ni-Mn-Co lithium-ion battery are used to validate the proposed approach. (4) Host computer: it is used to control the Arbin instrument and monitor the measured data.

The original specifications of the tested cells are listed in Table 2. The LFP lithium-ion cell uses the graphite as its negative electrode and lithium iron phosphate LiFePO4 as its positive electrode. Different from LFP, the NMC cell uses lithium iron phosphate Ni-Co-Mn as its positive electrode. The lithium-ion cells are placed in the thermal chamber. The characterization tests include standard capacity tests, OCV tests and the driving condition tests. The driving schedules are listed in Table 2. The aim of the capacity experiment is to determine the maximum available capacity (MAC) of the cell, which can be used to calibrate the reference SOC in OCV test. It is noticed that the MAC is dependent on the

TABLE 2. Basic parameters and testing condition of lithium-ion cells.

Battery type	LFP Cell	NMC Cell
Nominal voltage	3.2 V	3.65 V
Upper cutoff voltage	3.65 V	4.25 V
Lower cutoff voltage	2.5V	3.0 V
Nominal capacity	27 Ah	50 Ah
Working schedules	CTCDC−NEDC	UDDS−NEDC

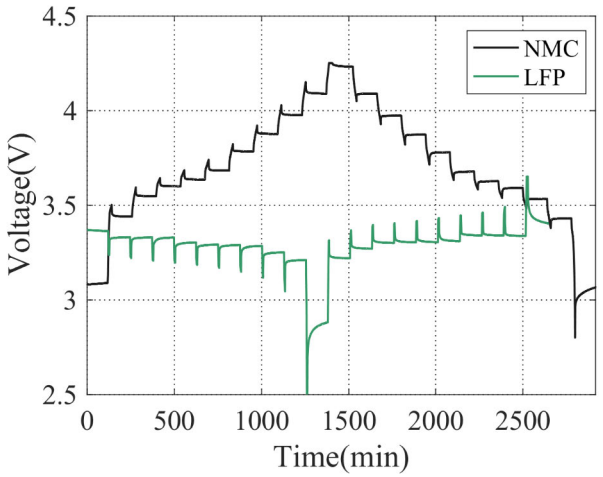

FIGURE 2. The OCV tests for the two batteries.

current, temperature and cycle state. The OCV experiment is used to determine the function between OCV and SOC. This test usually takes a long time to acquire the accurate function. Fig. 2 shows the OCV test results for the two types of batteries. The OCV of LFP is very flat in the middle SOC range, which is the main reason that the accuracy of SOC estimation deteriorates.

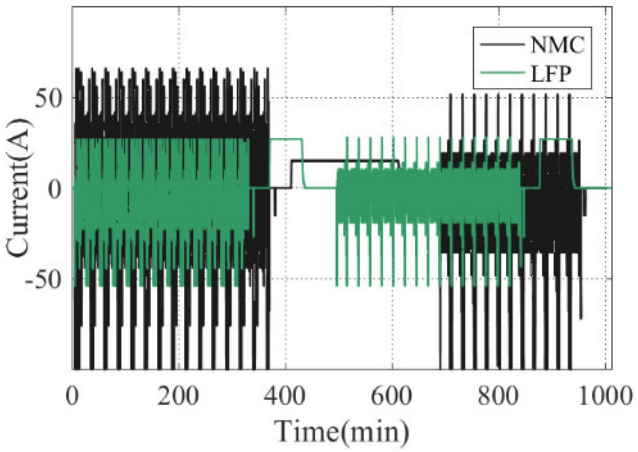

FIGURE 3. The working condition tests for batteries.

B. VERIFICATION BASED ON EXPERIMENTAL DATA

To verify the presented method, we test two types of batteries via some special current profiles which extract from the driving cycles, named Chinese Typical City Driving Cycle (CTCDC), New European Driving Cycle (NEDC), Urban Dynamometer Driving Schedule (UDDS) shown

in Fig. 3 [31], [32]. The operating SOC range is from 100% to 10% considering the practical application [33]. According to the actual capacity influence for SOC estimation, the initial capacity error in algorithm can be used to validate the robustness and reliability. Additionally, the SOC initial error is also taken into account to test the convergence of TVDSMO. To prove the advantages of TVDSMO, we compare it with ampere-hour integration and DSMO. Both of two observer-based methods have the same erroneous parameters listed in Table 3. For example, the true capacity of LFP under temperature 25 °C is 28Ah. The values of C_a are both set 25Ah in three algorithms. The same battery model is also used in the DSMO, whose parameters in Table 4 are determined by the optimization algorithm, such as the genetic algorithm. It is obvious that the maximum voltage errors (MVE) will increase in lower temperature. [34]. The results are listed in Table 4.

TABLE 3. The parameters in DSMO and TVDSMO.

Index	SOC initial error (reference/initial value)	Capacity initial error (reference/initial value)
LFP at 25°C	10%(100%/90%)	10.7%(28Ah/25Ah)
LFP at 10°C	10%(100%/90%)	10%(20Ah/18Ah)
NMC at 25°C	50%(100%/50%)	11.76%(51Ah/45Ah)
NMC at 10°C	50%(100%/50%)	11.8%(45Ah/40Ah)

TABLE 4. Parameters of the Thevenin model used in DSMO.

Index	$R_o(\Omega)$	$R_D(\Omega)$	$C_D(F)$	MVE(V)
LFP at 25°C	0.0016	0.0018	7467.41	0.0403
LFP at 10°C	0.0072	0.0080	2100.47	0.2859
NMC at 25°C	0.0011	0.0010	16749.69	0.0388
NMC at 10°C	0.0024	0.0021	15696.30	0.0640

1) CASE 1: SOC ESTIMATION AT TEMPERATURE 25°C

Figs. 4 and 5 present the comparison of the SOC estimation results calculated by three methods TVDSMO, DSMO and AHI at 25 °C. The root-mean square errors (RMSE), mean absolute errors (MAE), and maximum absolute errors (MAE) and convergence times (CT) are chosen to assess the performance of algorithms. The estimation results of LFP battery shown in Fig.5 indicate that the presented method can well deal with the variable parameters during the TVDSMO operation. The SOC estimation errors of CTCDC are within ±3.1%. The results of DSMO also can converge to the true value, but the MAE is larger than TVDSMO. The MAE of AHI is up to 10%. Additionally, the errors of TVDSMO increase during the NEDC condition, because the maximum discharge current (MDC) is different from the CTCDC. The MDC may cause the measurement noise of current sensors changing, which can lead errors to increase. This phenomenon also appears in the NMC battery. Additionally, the estimation errors of SOC do not increase when the initial capacity value set in TVDSMO diminishes. It shows the TVDSMO can well balance the model and measurement to restrain the raising tendency of error, different from the

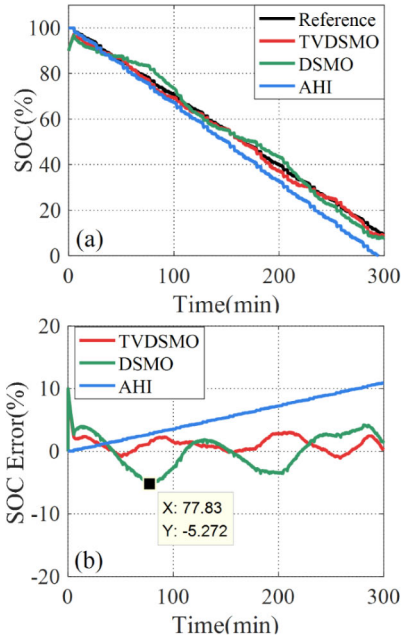

FIGURE 4. Experiments of an LFP battery from CTCDC under 25 °C: (a) SOC estimation results; (b) the estimation error.

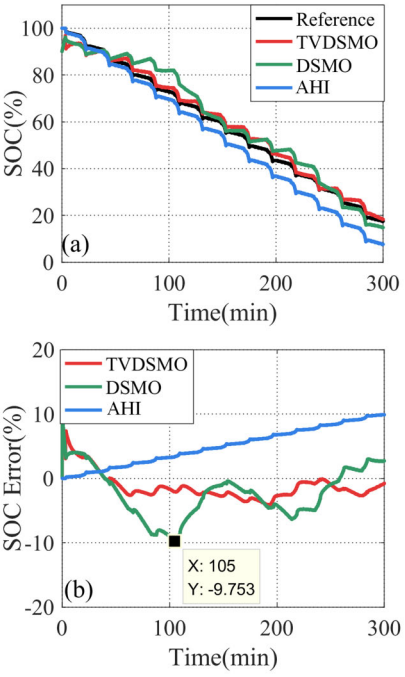

FIGURE 5. Experiments of an LFP battery from NEDC under 25 °C: (a) SOC estimation results, (b) the estimation error.

ampere-hour integration. Although the errors of DSMO do not increase during the testing condition, the MAE is worse than TVDSMO. The main reason is that the time-invariant model does not trace the dynamic behavior of LIBs.

Figs. 6 and 9 illustrate the stability of SOC estimation from different batteries under temperature 25°C , which shows that whether the values of gain are suitable for the operating condition during the iteration procedure of TVDSMO. The values are both positive during the whole process.

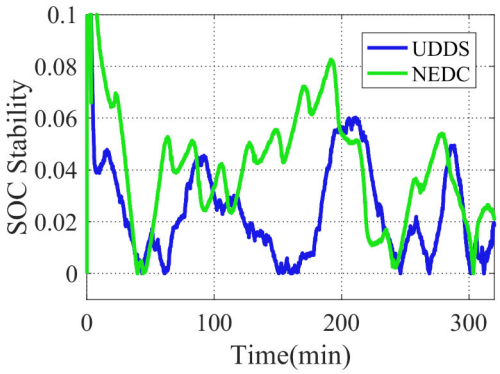

FIGURE 6. The stability of SOC estimation from LFP under temperature 25 °C.

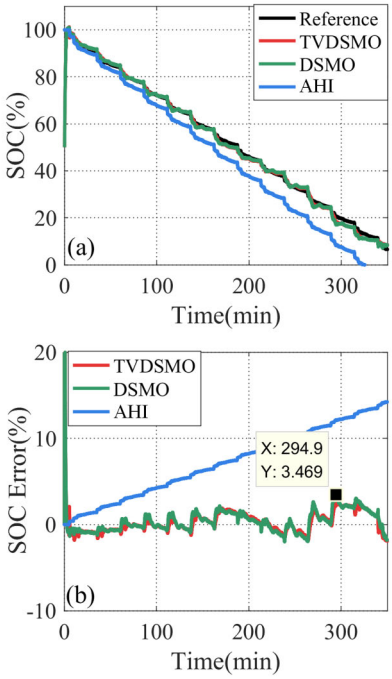

FIGURE 7. Experiments of an NMC battery from UDDS under temperature 25 °C: (a) SOC estimation results, (b) the estimation error.

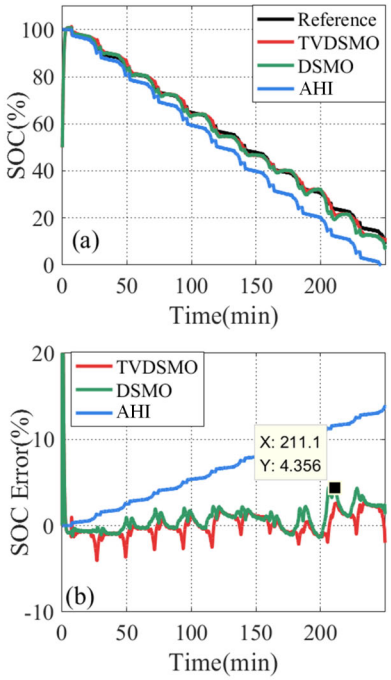

FIGURE 8. Experiments of an NMC battery from NEDC under 25 °C: (a) SOC estimation results, (b) the estimation error.

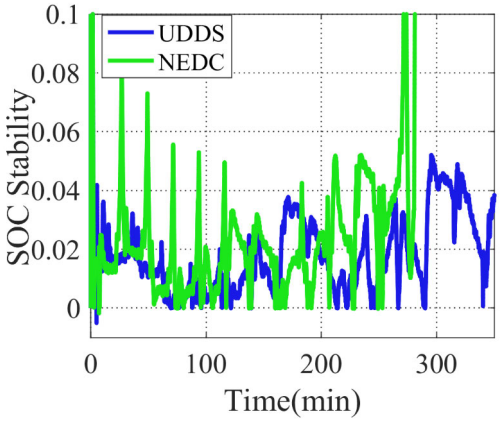

FIGURE 9. The stability of SOC estimation from NMC under temperature 25 °C.

Consequently, according to the condition of stability for discrete system, the chosen gains meet this condition.

Figs.7 and 8 are the comparison of the SOC estimation for NMC batteries estimated by three methods. The MAE from TVDSMO under UDDS is bigger than NEDC, which indicates the operation condition will change the accuracy for this method. Before application in the onboard controller of EVs, the working condition needs to be further investigated. And the parameters of TVDSMO need be matched. The CTs of the disparate operating conditions are very similar, but it is different for LFP. The CT of the proposed method may depend on the types of batteries. Because LFP has a very flat OCV during middle SOC range. The estimation errors of DMOS also are larger than TVDSMO. The MAEs of DSMO under both working conditions are 3.469% and 4.356%, respectively. Consequently, the TVDSMO has a better performance than the DMSO. Especially, the distinctions are more obvious during the large scale current loadings.

2) CASE 2: SOC ESTIMATION AT TEMPERATURE 10°C

Figs. 10, 11 and 12 demonstrate the comparison results of the SOC estimation calculated by TVDSMO, DSMO and AHI at 10°C. Fig. 10 shows the estimated results of LFP battery under UDDS. The MAE from TVDSMO is 2.61%, MEE is 1.12% and RMSE is 1.33%. The CT is about 1519 step. Usually, the SOC initial value will be calibrated during the battery system debugging. Consequently, the rest time is adequate for TVDSMO to converge to the target value during the application. However, the estimation results of DSMO suffer from the divergence problem. The MAE is up to 18.76%. Compared the SOC estimation during normal temperature,

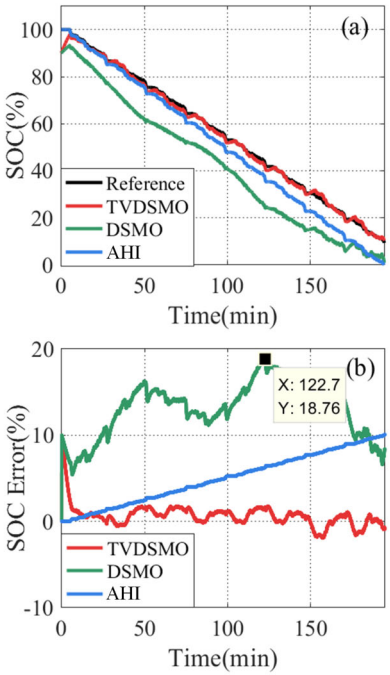

FIGURE 10. Verifications of LFP battery from CTCDC under 10°C: (a) SOC estimation results, (b) the estimation error.

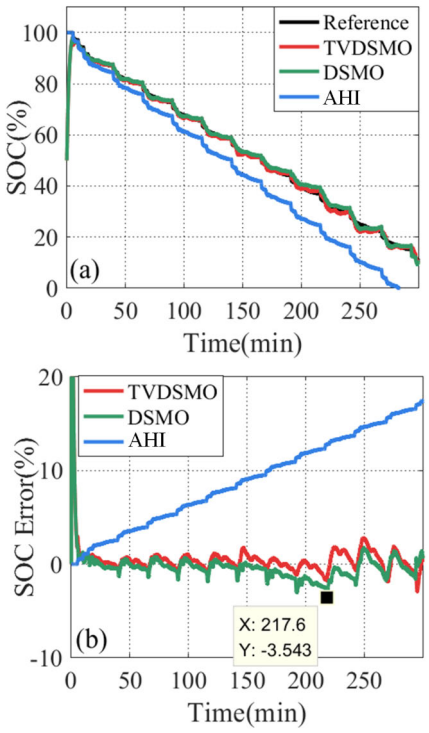

FIGURE 11. Verifications of NMC battery from UDDS under 10°C: (a) SOC estimation results, (b) the estimation error.

this method is distinctly inapplicable for LFP cells under lower temperature.

Fig. 11 shows the estimated results of NMC battery from UDDS. The MAE from TVDSMO is 3.1%, MEE is 0.6% and RMSE is 0.83%. The CT is 261 step times for converging to 3%. Fig. 12 shows the estimated results from NEDC. The MAE is 3.51%, MEE is 1.1% and RMSE is 1.35%. The CT is 227 step times for converging to the reference value. The TVDSMO is appropriate for NMC to estimate SOC with uncertain capacity and SOC initial error. It can be noticed that the maximum error usually appears in the rear SOC range. It is not a coincidence because the error of model raises in this range [30]. However, the MAEs from DSMO under two working condition are −3.543% and −3.135%, respectively. The CT from TVDSMO is similar to DSMO, about 150 steps.

Consequently, based on the two cases under different temperatures, we can conclude that the TVDSMO has stronger robustness and is more accurate than DSMO under the same uncertain errors. It is suitable for NMC and LFP battery SOC estimation.

C. VERIFICATION BASED ON HARDWARE-IN-LOOP

In order to fully verify the effectiveness of the proposed algorithm, a platform of algorithm verification is built, as shown in Fig. 13. The experimental platform includes: the Arbin BT2000, an ambient thermotank, the upper computer, a battery management system, Lithium-ion battery cells, and a power supply. The host computer mainly realizes the control of the Arbin instrument and monitor BMS data. The BMS includes BMU, BCU and current sensor. The BMS used in

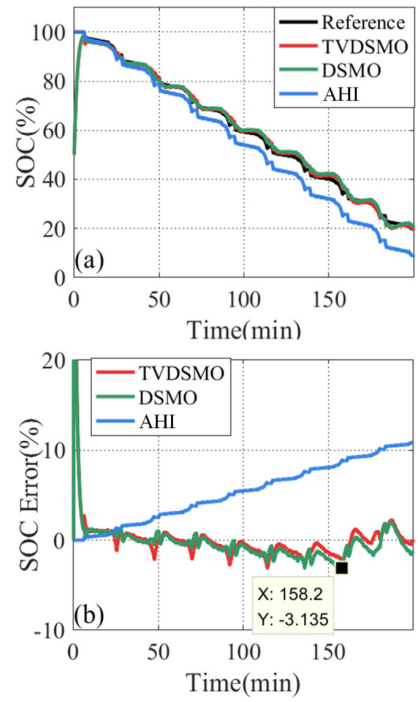

FIGURE 12. Verifications of NMC battery from NEDC under 10°C: (a) SOC estimation results,(b) the estimation error.

this paper was developed by our research group. Among them, the voltage acquisition chip adopts the mainstream LT6804 developed by Linear Technology. The maximum measurement error of the chip is less than 2mV. The core chip of BMU is MPC5644 from NXP. The calculation frequency

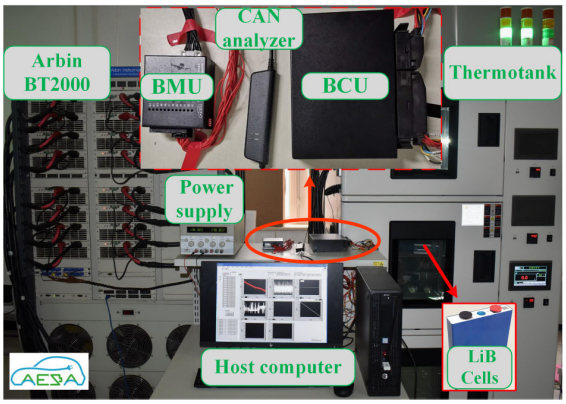

FIGURE 13. Hardware-in-loop verification platform.

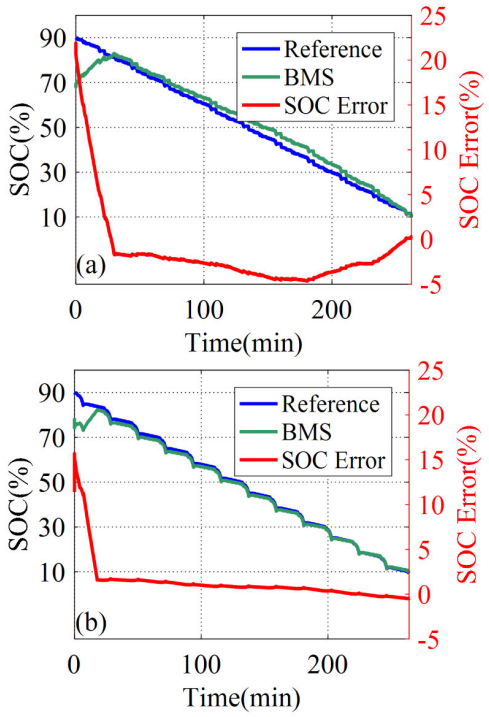

FIGURE 14. The results from the verification platform: (a) SOC results based on CTCDC, (b) SOC results based on NEDC.

used in this paper is 150Mhz. The BMU includes three-channel CAN bus, which can communicate with the vehicle controller, instrument and BMU. The presented algorithm to be verified is embedded in the controller.

The LFP battery cell mentioned above is adopted in the platform and the experiment temperature is 45°C. The OCV-SOC curve used in the BMS is the same as 25°C. The error of capacity is 10%. The real capacity is 27.98Ah and the value in BMS is set to 25Ah. To verify the convergence of the algorithm, the SOC of the battery is adjusted to 90%. CTCDC and NEDC conditions are performed during experiment. The estimation result of the CTCDC condition is shown by Fig. 14 (a). The initial value of the SOC in the algorithm is set to 70%, and the true value is 90%. The results show that the maximum error of this condition is 4.6%. The estimated SOC of the NEDC condition is shown in Fig. 14(b). The initial value of the SOC of the algorithm is 80%, and the true value is 90%. The results show that the maximum error of this condition is 1.9%. Since the OCV of the battery is relatively flat at 90%, the convergence speed is slow. In general, the algorithm meets the application of the BMS, and the calculation accuracy meets the requirements of the real vehicle.

V. CONCLUSIONS

In this paper, an improved time-varying-model-based discrete sliding mode observer is designed to estimate SOC. After the detailed discussion and analysis, We come to the following conclusions:

(1) The proposed method is applicable for different operating conditions and temperatures. The SOC simulation errors of LFP data under two temperatures are both within 3.1%. The SOC simulation errors of NMC cell are within 3%. Due to the slight difference of estimation results under different conditions and cells, it's a suggestion that parameters of TVDSMO should be further debugged under different working conditions before applying the algorithm. As the parameters of battery depending on the capacity degradation, the inaccurate capacity and SOC initial value need be considered. In this paper, the results of the show that the TVDSMO has better robustness and accuracy than DSMO at different temperatures. Its accuracy is still within 4% with the 10% capacity error.

(2) The stability of the presented algorithm should be validated before using it. For the discrete system with time-varying parameters, we suggest using the proposed stability condition to validate stability.

(3) To test the applicability of the proposed algorithm, we build a hardware verification platform. The verification results of the actual BMS show that the SOC errors are less than 4.6%.

ACKNOWLEDGMENT

The systematic experiments of the lithium-ion batteries were performed at the Advanced Energy Storage and Application (AESA) Group, Beijing Institute of Technology.

REFERENCES

[1] L. Lu, X. Han, J. Li, J. Hua, and M. Ouyang, "A review on the key issues for lithium-ion battery management in electric vehicles," *J. Power Sour.*, vol. 226, pp. 272–288, Mar. 2013.

[2] M. A. Hannan, M. S. H. Lipu, A. Hussain, and A. Mohamed, "A review of lithium-ion battery state of charge estimation and management system in electric vehicle applications: Challenges and recommendations," *Renew. Sustain. Energy Rev.*, vol. 78, pp. 834–854, Oct. 2017.

[3] W. Waag, C. Fleischer, and D. U. Sauer, "Critical review of the methods for monitoring of lithium-ion batteries in electric and hybrid vehicles," *J. Power Sour.*, vol. 258, pp. 321–339, Jul. 2014.

[4] R. Xiong, J. Cao, Q. Yu, H. He, and F. Sun, "Critical review on the battery state of charge estimation methods for electric vehicles," *IEEE Access*, vol. 6, pp. 1832–1843, 2017.

[5] P. Shen, M. Ouyang, L. Lu, J. Li, and X. Feng, "The co-estimation of state of charge, state of health, and state of function for lithium-ion batteries in electric vehicles," *IEEE Trans. Veh. Technol.*, vol. 67, no. 1, pp. 92–103, Jan. 2018.

[6] Z. Li, J. Huang, B. Y. Liaw, and J. Zhang, "On state-of-charge determination for lithium-ion batteries," *J. Power Sources*, vol. 348, pp. 281–301, Apr. 2017.
[7] R. Yang, R. Xiong, H. He, H. Mu, and C. Wang, "A novel method on estimating the degradation and state of charge of lithium-ion batteries used for electrical vehicles," *Appl. Energy*, vol. 207, pp. 336–345, Dec. 2017.
[8] J. Wang, R. Xiong, L. Li, and Y. Fang, "A comparative analysis and validation for double-filters-based state of charge estimators using battery-in-the-loop approach," *Appl. Energy*, vol. 229, pp. 648–659, Nov. 2018.
[9] M. A. Roscher and D. U. Sauer, "Dynamic electric behavior and open-circuit-voltage modeling of $LiFePO_4$-based lithium ion secondary batteries," *J. Power Sources*, vol. 196, no. 1, pp. 331–336, 2011.
[10] Y. Zheng, M. Ouyang, X. Han, L. Lu, and J. Li, "Investigating the error sources of the online state of charge estimation methods for lithium-ion batteries in electric vehicles," *J. Power Sources*, vol. 377, pp. 161–188, Feb. 2018.
[11] E. Chemali, P. J. Kollmeyer, M. Preindl, R. Ahmed, and A. Emadi, "Long short-term memory networks for accurate state-of-charge estimation of Li-ion batteries," *IEEE Trans. Ind. Electron.*, vol. 65, no. 8, pp. 6730–6739, Aug. 2018.
[12] J. Xu, C. C. Mi, B. Cao, J. Deng, Z. Chen, and S. Li, "The state of charge estimation of lithium-ion batteries based on a proportional-integral observer," *IEEE Trans. Veh. Technol.*, vol. 63, no. 4, pp. 1614–1621, May 2014.
[13] G. L. Plett, "Extended Kalman filtering for battery management systems of LiPB-based HEV battery packs: Part 3. State and parameter estimation," *J. Power Sources*, vol. 134, no. 2, pp. 277–292, 2004.
[14] R. Xiong, F. Sun, X. Gong, and C. Gao, "A data-driven based adaptive state of charge estimator of lithium-ion polymer battery used in electric vehicles," *Appl. Energy*, vol. 113, pp. 1421–1433, Jan. 2014.
[15] G. L. Plett, "Sigma-point Kalman filtering for battery management systems of LiPB-based HEV battery packs: Part 2: Simultaneous state and parameter estimation," *J. Power Sources*, vol. 161, no. 2, pp. 1369–1384, 2006.
[16] J. K. Barillas, J. Li, C. Günther, and M. A. Danzer, "A comparative study and validation of state estimation algorithms for Li-ion batteries in battery management systems," *Appl. Energy*, vol. 155, pp. 455–462, Oct. 2015.
[17] F. Zhang, G. Liu, and L. Fang, "A battery state of charge estimation method using sliding mode observer," in *Proc. 7th World Congr. Intell. Control Automat.*, Jun. 2008, pp. 989–994.
[18] I.-S. Kim, "The novel state of charge estimation method for lithium battery using sliding mode observer," *J. Power Sour.*, vol. 163, no. 1, pp. 584–590, 2006.
[19] Y. G. Huangfu, J. N. Xu, S. R. Zhuo, M. C. Xie, and Y. T. Liu, "A novel adaptive sliding mode observer for SOC estimation of lithium batteries in electric vehicles," in *Proc. PESA*, 2017, pp. 1–6.
[20] X. Chen, W. X. Shen, Z. Cao, and A. Kapoor, "Sliding mode observer for state of charge estimation based on battery equivalent circuit in electric vehicles," *Austral. J. Elect. Electron. Eng.*, vol. 9, no. 3, pp. 225–234, 2012.
[21] W. Li, L. Liang, W. Liu, and X. Wu, "State of charge estimation of lithium-ion batteries using a discrete-time nonlinear observer," *IEEE Trans. Ind. Electron.*, vol. 64, no. 11, pp. 8557–8565, Nov. 2017.
[22] J. Du, Z. Liu, Y. Wang, and C. Wen, "An adaptive sliding mode observer for lithium-ion battery state of charge and state of health estimation in electric vehicles," *Control Eng. Pract.*, vol. 54, pp. 81–90, Sep. 2016.
[23] Q. Zhong, F. Zhong, J. Cheng, H. Li, and S. Zhong, "State of charge estimation of lithium-ion batteries using fractional order sliding mode observer," *ISA Trans.*, vol. 66, pp. 448–459, Jan. 2017.
[24] B. Ning, B. Cao, B. Wang, and Z. Zou, "Adaptive sliding mode observers for lithium-ion battery state estimation based on parameters identified online," *Energy*, vol. 153, pp. 732–742, Jun. 2018.
[25] Z. Wei, S. Meng, B. Xiong, D. Ji, and K. J. Tseng, "Enhanced online model identification and state of charge estimation for lithium-ion battery with a FBCRLS based observer," *Appl. Energy*, vol. 181, pp. 332–341, Nov. 2016.
[26] I.-S. Kim, "A technique for estimating the state of health of lithium batteries through a dual-sliding-mode observer," *IEEE Trans. Power Electron.*, vol. 25, no. 4, pp. 1013–1022, Apr. 2010.
[27] V. Sharma and B. Pratap, "Sliding mode observer based controller of uncertain systems: An LMI based approach," in *Proc. 2nd Int. Conf. Power, Control Embedded Syst.*, Dec. 2012, pp. 1–5.
[28] S. Sarpturk, Y. Istefanopulos, and O. Kaynak, "On the stability of discrete-time sliding mode control systems," *IEEE Trans. Autom. Control*, vol. 32, no. 10, pp. 930–932, Oct. 1987.
[29] T. M. Bond, J. C. Burns, D. A. Stevens, H. M. Dahn, and J. R. Dahn, "Improving precision and accuracy in coulombic efficiency measurements of Li-ion batteries," *J. Electrochem. Soc.*, vol. 160, no. 3, pp. A521–A527, 2013.
[30] R. Xiong, J. Tian, F. Sun, and W. Shen, "A novel fractional order model for state of charge estimation in lithium ion batteries," *IEEE Trans. Veh. Technol.*, vol. 68, no. 5, pp. 4130–4139, May 2019.
[31] R. Xiong, Y. Zhang, H. He, S. Peng, M. Pecht, and J. Wang, "Lithium-ion battery health prognosis based on a real battery management system used in electric vehicles," *IEEE Trans. Veh. Technol.*, vol. 68, no. 5, pp. 4110–4121, May 2019.
[32] R. Xiong, H. Chen, C. Wang, and F. Sun, "Towards a smarter hybrid energy storage system based on battery and ultracapacitor—A critical review on topology and energy management," *J. Cleaner Prod.*, vol. 202, pp. 1228–1240, Nov. 2018.
[33] R. Xiong, J. Cao, and Q. Yu, "Reinforcement learning-based real-time power management for hybrid energy storage system in the plug-in hybrid electric vehicle," *Appl Energy*, vol. 211, pp. 538–548, Feb. 2018.
[34] R. Xiong, L. Li, Z. Li, Q. Yu, and H. Mu, "An electrochemical model based degradation state identification method of Lithium-ion battery for all-climate electric vehicles application," *Appl. Energy*, vol. 219, no. 5, pp. 264–275, Jun. 2018.

KANGWEI DAI received the Ms.E. degree in vehicle engineering from the Hefei University of Technology, China, in 2008. She is currently pursuing the Ph.D. degree in vehicle engineering with the National Engineering Laboratory for Electric Vehicles, Beijing Institute of Technology, Beijing, China.

Her research mainly focuses on SOC and SOE estimation of lithium ion batteries.

JU WANG received the Ms.E. degree in automotive engineering from the Beijing Institute of Technology, Beijing, China, in 2017. He is currently pursuing the Ph.D. degree in vehicle engineering with the National Engineering Laboratory for Electric Vehicles, Beijing Institute of Technology and Collaborative Innovation Center of Electric Vehicles in Beijing, China.

His research mainly focuses on multi-state estimation of lithium ion batteries and battery management system design.

HONGWEN HE (M'03–SM'12) received the Ms.E. degree from the Jilin University of Technology, Changchun, China, in 2000, and the Ph.D. degree from the Beijing Institute of Technology, Beijing, China, in 2003, both in vehicle engineering.

He is currently a Professor with the National Engineering Laboratory for Electric Vehicles, School of Mechanical Engineering, Beijing Institute of Technology. He has published more than 100 papers and holds 20 patents. His research interests include power battery modeling and simulation on electric vehicles, design, and control theory of the hybrid power trains.

Dr. He was a recipient of the second prize of the Chinese National Science and Technology Award for the work on the development of new-energy electric bus powertrains, in 2015, the first prize of the Henan Science and Technology Award for the work on the development of hybrid bus powertrain, in 2013, the first prize of the Henan Science and Technology Award for the work on the development of battery electric bus powertrain, in 2014, and the second prize of the MIIT Technology Innovation Award for the work on the development of hybrid powertrains in off road vehicles, in 2016.